An SPH Approach for Fluid-Hypoelastic Structure Interactions with Free Surfaces

Nima Amanifard, Muhammad Hesan, Behnam Rahbar

***Abstract*—This contribution presents a numerical method for the analysis of fluid-hypoelastic structure interaction (FSI) problems with free surface flows. The fluid is fully coupled with the structures which can undergo large structural displacements, rotations and deformations. The employed smoothed particle hydrodynamics (SPH) algorithm consists of three steps. The first two steps play the role of prediction, while in the third step a Poisson equation is used for both fluid and structure. To alleviate the numerical difficulties encountered when a hypoelastic solid structure is highly stretched, an artificial stress term is incorporated into the momentum equation which reduces the risk of unrealistic fractures in the material. The implemented scheme is used to solve three fluid structure interaction problems including breaking of a column of water on a rigid wall, breaking dam on a hypoelastic baffle, and bar under a lateral wave.**

***Index Terms*—Smoothed particle hydrodynamics (SPH), Fluid-structure interaction (FSI), Hypoelasticity, Artificial stress**

I. Introduction

COMPUTATIONAL simulation of the fluid flow has been well developed mostly based on the mesh-based methods. Conventional mesh-based numerical methods such as FDM and FEM have been widely applied to various computational fluid and solid dynamics (CFD and CSD), and currently are the dominant methods in numerical simulations of domain discretization and numerical discretization. Mesh based methods were first divided into two groups based on two fundamental frames for describing the physical governing equations: Eulerian (e.g., FDM) and Lagrangian (e.g., FEM) descriptions. Each of them has some advantages and disadvantages.

For example using traditional methods such as FEM might cause some difficulties like: tracking the position of an interface or free surfaces, and information transfer between the fluid and the structure domains. The different but complementary features of the Lagrangian and Eulerian descriptions suggest that it would be computationally beneficial to combine these two descriptions. This idea has led to two complicated approaches: Coupled Eulerian Lagrangian (CEL) and the Arbitrary Lagrange Eulerian (ALE) [1,2,3].

Many numerical methods where suggested to solve multiphysics problems and large number of techniques have been proposed to analyze engineering problems involving the interaction of fluids and structures (FSI). ALE methods are most commonly used for these problems. However this method does not suffice for large deformations, translations and rotations of solid.

In general, there are two classes of fluid-structure coupling, namely staggered (or partitioned, or iterative) and direct (or simultaneous, or monolithic) approaches.

If the interaction of an elastic body and fluid flows is slight, (e.g., blood flow in elastic arteries), a loose or weak coupling may be adequate. However it is still difficult to analyze problems like free surface flows and fluid-hypoelastic structure interactions where the structure undergoes large displacements, rotations and deformations. Examples of this kind are common in ship hydrodynamics, off-shore structures, spill-ways in dams, free surface channel flows, liquid containers, mould filling processes, biomedical engineering applications like dynamics of heart valves, blood flow in arteries and etc. Considering these wide fields of applications for FSI problems, they have been given increased attention during recent years.

In staggered schemes, solvers of different continua are separately applied and interactions are taken into account at the interfaces. This scheme is ideal for using existing finite element codes, initially developed for fluid dynamics and solid mechanics problems, and the computing effect is mainly focused on the interfacing of the relevant data between the common fluid and solid boundaries. In the case of monolithic techniques all continua are considered as a unique system, hence, it is usually included an implicit time-integration in which boundaries are considered.

As mentioned before, mesh-based methods suffer from some inherent difficulties in many aspects, which limit their applications to many problems. A very preferred numerical method to simulate large deformations is smoothed particle hydrodynamics (SPH) which is a meshfree, lagrangian, particle method. In the SPH method, the state of a system is represented by a set of particles, which possess individual material properties and move according to the governing equations. Since its invention to solve astrophysical problems in three-dimensional open space (Lucy [4], Gingold and Monaghan [5]), SPH has been extensively studied and extended to dynamic response with material strength as well as dynamic fluid flows with large deformations.

Manuscript received March 5, 2011

N. Amanifard is Associated Professor in Department of Mechanical Engineering, Faculty of Engineering, University of Guilan, Rasht, 3756 IRAN (Corresponding author; phone: 98-131-6690274-8; fax: 98-131-6690271; e-mail: namanif@guilan.ac.ir).

M. Hesan is with Department of Mechanical Engineering, Faculty of Engineering, University of Guilan, Rasht, 3756 IRAN (e-mail: Muh.Hesan@yahoo.com).

B. Rahbar is with Department of Mechanical Engineering, Faculty of Engineering, University of Guilan, Rasht, 3756 IRAN (e-mail: B.Rahbar@msc.guilan.ac.ir).

ISBN: 978-988-19251-5-2
ISSN: 2078-0958 (Print); ISSN: 2078-0966 (Online)

The word "particle" does not mean a physical mass instead it refers to a region in space. Field variables are associated with these particles and at any other point in space are found by averaging or smoothing, the values over the region of interest. This is fulfilled by an interpolation or weight function which is often called the interpolation kernel.

SPH was successfully applied to the study of various fluid dynamic problems, e.g., free surface incompressible flows, viscous flows, and viscoelastic free surface flows (review articles by Monaghan are useful literature reviews for SPH method [6,7]). Antoci *et al.* (2007) used a weakly compressible SPH method for the simulation of FSI [8].

A different route for solving FSI problems is using a so-called Particle Finite Element Method (PFEM) by Idelsohn *et al* [9]. This method allows treating the fluid and the solid as a single entity and treats the mesh nodes in the fluid and solid domain as particle which can freely move and even separate from the main fluid domain.

In the current work, FSI simulation with complex free surface flows is studied and three benchmark problems are solved: breaking of a column of water on a rigid wall, breaking dam on hypoelastic baffle and bar under a lateral wave.

II. Governing equations

The governing equations of transient compressible fluid flow include the equations for conservation of mass and momentum. In a lagrangian framework these can be written as:

$$\frac{1}{\rho}\frac{D\rho}{Dt}+\frac{\partial u^{\alpha}}{\partial x^{\alpha}}=0. \tag{1}$$

$$\frac{Du^{\alpha}}{Dt}=g^{\alpha}+\frac{1}{\rho}\frac{\partial \tau^{\alpha\beta}}{\partial x^{\alpha}}-\frac{1}{\rho}\frac{\partial P}{\partial x^{\alpha}} \tag{2}$$

where t is time, g is gravitational acceleration, P is pressure, α and β refer to the spatial coordinates and u is the velocity vector. Note that the material derivative D/Dt is equal to $\partial/\partial t+u.\nabla$. The density ρ has been intentionally kept in the equations to be able to enforce the incompressibility of the fluid. It also facilitates coupling between the pressure and velocity fields.

The acceleration equations (momentum equation) of elastic dynamics can be written as below:

$$\frac{Du^{\alpha}}{Dt}=\frac{1}{\rho}\frac{\partial \sigma^{\alpha\beta}}{\partial x^{\alpha}}+g^{\alpha} \tag{3}$$

In the above equation σ is the stress tensor and can be written as:

$$\sigma^{\alpha\beta}=-P\delta^{\alpha\beta}+S^{\alpha\beta} \tag{4}$$

In the above equation $S^{\alpha\beta}$ is deviatoric stress. Substituting equation (4) into equation (3) yields

$$\frac{Du^{\alpha}}{Dt}=\frac{1}{\rho}\frac{\partial S^{\alpha\beta}}{\partial x^{\alpha}}-\frac{1}{\rho}\frac{\partial P}{\partial x^{\alpha}}+g^{\alpha} \tag{5}$$

For solids, the linear elastic relation between stress and deformation tensors can be derived in time in order to obtain an evolution equation for $S^{\alpha\beta}$. The use of corotational, or Jaumann time derivative guarantees that formulation is independent from superposed rigid rotations, resulting in the incremental formulation of Hook's law corrected by Jaumann rate.

$$\frac{DS^{\alpha\beta}}{Dt}=2G\left(\dot{\varepsilon}^{\alpha\beta}-\frac{1}{3}\dot{\varepsilon}^{\alpha\beta}\delta^{\alpha\beta}\right)+S^{\alpha\beta}\omega^{\beta\gamma}+\omega^{\alpha\gamma}S^{\gamma\beta} \tag{6}$$

where G is the shear modulus. The strain rate tensor $\dot{\varepsilon}^{\alpha\beta}$ and rotation tensor $\omega^{\alpha\beta}$ are defined as:

$$\dot{\varepsilon}^{\alpha\beta}=\frac{1}{2}\left(\frac{\partial u^{\alpha}}{\partial x^{\beta}}+\frac{\partial u^{\beta}}{\partial x^{\alpha}}\right) \tag{7}$$

$$\omega^{\alpha\beta}=\frac{1}{2}\left(\frac{\partial u^{\alpha}}{\partial x^{\beta}}-\frac{\partial u^{\beta}}{\partial x^{\alpha}}\right) \tag{8}$$

Despite having disadvantage that energy is not conserved in the case of large deformations, the method has the advantage of common descriptive of both fluid and solid dynamics in terms of pressure and velocity.

III. SPH method

A. Integral Representation of a Function

The SPH method is based on the interpolation theory. The formulation of SPH is often divided into two key steps. The first step is the *integral representation* or so-called *kernel approximation* of field functions. The second one is the *particle approximation*.

In the first key step, the integration of multiplication of an arbitrary function and a smoothing kernel function gives the kernel approximation. The concept of integral representation of a function F(r) used in the SPH method starts from the following identity

$$F(r)=\int_{V}F(r')\delta(r-r')dr' \tag{9}$$

where δ(r-r') is the Dirac delta function, V is the computational domain and r is the position vector. If the Dirac delta function is replaced by a smoothing kernel function W(r-r',h), the integral representation of F(r) is given by

$$F(r)\approx\int_{V}F(r')W(r-r',h)dr' \tag{10}$$

where h is the smoothing length defining the influence area of the weighting or smoothing function W. Note that as long as W is not the Dirac function, the integral representation in (10) can only be an approximation.

In the SPH method, the entire system is represented by a finite number of particles that carry individual mass and occupy individual space. This is achieved by the following *particle approximation*, which is another key operation in the SPH method. Particle approximation of a function and its derivative are carried out using discretized particles in the support domain. If F(r') is known only at discrete set of N points r_1, r_2, …, r_N then F(r') can be approximated as follows

$$F_h(r)=\sum_{b=1}^{N}\frac{m_b}{\rho_b}F_bW(r-r',h) \tag{11}$$

where the summation index b denotes a particle label and particle b carries a mass m_b at the position r_b. The value of F at b-th particle is shown by F_b.

ISBN: 978-988-19251-5-2
ISSN: 2078-0958 (Print); ISSN: 2078-0966 (Online)

B. Kernel Function

The smoothing kernel function W is usually chosen to be an even function and it should also satisfy a number of conditions

$$\begin{cases} \int_V W(r-r',h)dr' = 1 \\ \lim_{h\to 0} W(r-r',h) = \delta(r-r') \\ W(r-r',h) = 0 \xrightarrow{when} |r-r'| > \kappa h \end{cases} \tag{12}$$

The first condition is called *normalization condition* or *unity condition* and the second one is *Delta function property* that is observed when the smoothing length approaches zero. The third one is *compact condition* where κ is a constant related to the smoothing function for point at r, and defines the effective (non-zero) area of the smoothing function. This effective area is called the support domain for the smoothing function of point r.

Recent studies indicate that the stability of the SPH algorithm depends strongly upon the second derivative of the kernel [10]. Various forms have been proposed for kernel function, ranging from Gaussian functions, to spline function. In fact the cubic spline is the most frequently used kernel and in comparison with quintic kernel (one of the most famous Gaussian functions) has a smaller compact support which lower amount of computation effort should be carried out. In this paper a popular kernel is used which was devised by Monaghan and Lattanzio [11]. They formulated the following smoothing function based on the cubic spline functions known as the B-spline function

$$W(r,h) = \frac{\Psi}{h^{\nu}} \begin{cases} 1 - 1.5s^2 + 0.75s^3 & 0 \le s < 1 \\ 0.25(2-s)^3 & 1 \le s < 2 \\ 0 & 2 \le s \end{cases} \tag{13}$$

where s=|r|/h , υ is number of dimensions and Ψ is normalization constant with the values: 2/3, 10/7π, 1/π in one, two and three dimensional respectively.

Although by increasing the number of neighboring particles the accuracy of the SPH method can be improved, the computational expenses also increase sharply. Numerical experiences have shown that a total number of neighboring particles between 20 and 30 is good compromise for two dimensional problems.

C. Tensorial Operators

There are two commonly used forms for gradient of a scalar F in the SPH contexts. In this paper first formulation is used.

$$\frac{1}{\rho_a}\nabla_a F = \sum_b m_b \left(\frac{F_a}{\rho_a^2} + \frac{F_b}{\rho_b^2} \right) \nabla_a W_{ab} \tag{14}$$

$$\frac{1}{\rho_a}\nabla_a F = \sum_b m_b \left(\frac{F_a + F_b}{\rho_a \rho_b} \right) \nabla_a W_{ab} \tag{15}$$

where ∇_a means the gradient with respect to coordinates of particle a and $\nabla_a W_{ab}$ is the gradient of the kernel function $W(|r_a-r_b|,h)$ with respect to r_a, the position of particle a.

$$\nabla_a W_{ab} = \nabla_a W(r_a - r_b, h) = \frac{dW}{dr_{ab}} \frac{1}{|r_{ab}|} (x_a^{\alpha} - x_b^{\beta}) \tag{16}$$

There are also two commonly used forms for discretization of the Laplacian operator in the SPH contexts. In this paper first formulation is used.

$$\nabla.\left(\frac{1}{\rho}\nabla F \right)_a = \sum_b m_b \frac{8}{(\rho_a + \rho_b)^2} \frac{F_{ab} r_{ab} . \nabla_a W_{ab}}{|r_{ab}|^2 + \eta^2} \tag{17}$$

$$\nabla.\left(\frac{1}{\rho}\nabla F \right)_a = \sum_b \frac{m_b}{\rho_b} \frac{4}{(\rho_a + \rho_b)} \frac{F_{ab} r_{ab} . \nabla_a W_{ab}}{|r_{ab}|^2 + \eta^2} \tag{18}$$

where $F_{ab}=F_a-F_b$, $r_{ab}=r_a-r_b$ and η is a small number introduced to avoid a zero dominator during computations and is set to 0.1h.

D. Tensile instability

Equation (5) can be written in the following SPH form:

$$\frac{Du_a^{\alpha}}{Dt} = \sum_b m_b \left(\frac{S_a^{\alpha\beta}}{\rho_a^2} + \frac{S_b^{\alpha\beta}}{\rho_b^2} - \left(\frac{P_a}{\rho_a^2} + \frac{P_b}{\rho_b^2} \right) \delta^{\alpha\beta} \right) . \nabla_a W_{ab} + g^{\alpha} \tag{19}$$

By using the above form of momentum equation, a numerical instability known as "tensile instability" occurs. In the initial application of SPH it was noticed that, under tension particles tended to clump in pairs. Various methods have been proposed to eliminate it from SPH simulations. One of the most successful techniques is the "artificial stress" method due to Monaghan and Grey *et al.* [12] , the idea behind artificial stress is to add short-length repulsive force between two particles to prevent them from clustering together when they are in a state of tensile stress. Therefore the modified form of the equation (19) is in the following form, where l_0 is the initial particle spacing and R is artificial stress in the original coordinate system.

$$\frac{Du_a^{\alpha}}{Dt} = \sum_b m_b \left(\frac{S_a^{\alpha\beta}}{\rho_a^2} + \frac{S_b^{\alpha\beta}}{\rho_b^2} - \left(\frac{P_a}{\rho_a^2} + \frac{P_b}{\rho_b^2} \right) \delta^{\alpha\beta} + R_{ab}^{\alpha\beta} f_{ab}^n \right) . \nabla_a W_{ab} + g^{\alpha} \tag{20}$$

$$R_{ab}^{\alpha\beta} = R_a^{\alpha\beta} + R_b^{\alpha\beta} \quad and \quad f = W_{ab}/W(h, l_0)$$

If the angle of rotation for particle "a" is denoted by θ_a the stress tensor will be diagonal if

$$\theta_a = 0.5 * \tan^{-1}\left(\frac{2\sigma_a^{\alpha\beta}}{\sigma_a^{\alpha\alpha} - \sigma_a^{\beta\beta}} \right) \tag{21}$$

If c denotes $\cos\theta_a$ and s denotes $\sin\theta_a$, new components of the stress tensor for particle a, in the rotated frame are:

$$\begin{aligned} \overline{\sigma}_a^{\alpha\alpha} &= c^2 \sigma_a^{\alpha\alpha} + 2sc\,\sigma_a^{\alpha\beta} + s^2 \sigma_a^{\beta\beta} \\ \overline{\sigma}_a^{\beta\beta} &= s^2 \sigma_a^{\alpha\alpha} + 2sc\,\sigma_a^{\alpha\beta} + c^2 \sigma_a^{\beta\beta} \end{aligned} \tag{22}$$

Just for positive values of new components of stress tensor, artificial stress can be calculated as follows; otherwise artificial stress components are equal to zero.

$$\overline{R}_a^{\alpha\alpha} = -e \frac{\overline{\sigma}_a^{\alpha\alpha}}{\rho^2} \quad and \quad \overline{R}_a^{\beta\beta} = -e \frac{\overline{\sigma}_a^{\beta\beta}}{\rho^2} \tag{23}$$

where 0<e<1 is a parameter. Components of the artificial stress in the original coordinates for particle "a" are:

$$\begin{aligned} R_a^{\alpha\alpha} &= c^2 \overline{R}_a^{\alpha\alpha} + s^2 \overline{R}_a^{\beta\beta} \\ R_a^{\alpha\beta} &= sc\left(\overline{R}_a^{\alpha\alpha} - \overline{R}_a^{\beta\beta} \right) \\ R_a^{\beta\beta} &= s^2 \overline{R}_a^{\alpha\alpha} + c^2 \overline{R}_a^{\beta\beta} \end{aligned} \tag{24}$$

Gray *et al.* derived optimal values from the dispersion equations as e = 0.3 and n = 4.

ISBN: 978-988-19251-5-2
ISSN: 2078-0958 (Print); ISSN: 2078-0966 (Online)

IV. SOLUTION ALGORITHM

As mentioned before, in this work a three step prediction correction scheme is used to march in time. This algorithm is similar to the SPH projection method which was proposed by Cummins *et al.* [13], and the prediction-correction procedure of Shao *et al.* [14], with other modifications [15,16,17].

A. First Step (Prediction)

In the first step of this algorithm, the momentum equation is solved in the presence of the body forces. The computed provisional velocity is then used in the second step to calculate the divergence of shear stress tensor.

$$\bar{u}^{\alpha} = u^{\alpha}_{t-\Delta t} + g^{\alpha}\Delta t \tag{25}$$

B. Second Step (Prediction)

Fluid: In this step the divergence of shear stress tensor T_f^{α}, regardless of incompressibility is calculated.

$$T_f^{\alpha} = \left(\frac{1}{\rho}\frac{\partial \tau^{\alpha\beta}}{\partial x^{\beta}}\right)_a = \sum_b m_b \left(\frac{(\mu_a + \mu_b)(\bar{u}_a^{\alpha} - u_b^{\alpha})}{\rho_a \rho_b (r_{ab}^2 + \eta^2)}\right) x_{ab}^{\alpha}.\nabla_a W_{ab} \tag{26}$$

Solid: In this step the divergence of deviatoric stress tensor T_s^{α}, is calculated, where artificial stress is also considered.

$$T_s^{\alpha} = \left(\frac{1}{\rho}\frac{\partial S^{\alpha\beta}}{\partial x^{\beta}}\right)_a = \sum_b m_b \left(\frac{S_a^{\alpha\beta}}{\rho_a^2} + \frac{S_b^{\alpha\beta}}{\rho_b^2} + R_{ab}^{\alpha\beta} f_{ab}^{n}\right).\nabla_a W_{ab} \tag{27}$$

Fluid/Solid: At the end of the second step, an intermediate velocity and position for particles are obtained.

$$\bar{\bar{u}}^{\alpha} = \bar{u}^{\alpha} + T^{\alpha}\Delta t \tag{28}$$

$$\bar{x}^{\alpha} = x^{\alpha}_{t-\Delta t} + \bar{\bar{u}}^{\alpha}\Delta t \tag{29}$$

C. Third Step (Correction)

This step is common to both fluid and structure particles. So far no constraint has been imposed to satisfy the incompressibility of the fluid particles and it is expected that the density of some particles deviates from initial density (ρ_0) and is denoted as $\bar{\rho}$. This deviation can be calculated from following formula.

$$\left(\frac{d\bar{\rho}}{dt}\right)_a = \rho_a \sum_b \frac{m_b}{\rho_b}(\bar{\bar{u}}_a^{\alpha} - u_b^{\alpha}).\nabla_a W_{ab} \tag{30}$$

In the correction step the pressure Poisson equation is solved to enforce incompressibility. This equation is resulted from combination of the momentum equation (2) with the continuity equation (1).

$$\nabla.\left(\frac{1}{\bar{\rho}}\nabla P\right) = \frac{\rho_0 - \bar{\rho}}{\rho_0 \Delta t^2} \tag{31}$$

Previous equation can be discretized according to SPH Laplacian formulation, to obtain the pressure of each particle.

$$P_a = \left(\frac{\rho_0 - \bar{\rho}_a}{\rho_0 \Delta t^2} + \sum_b \frac{8m_b}{(\bar{\rho}_a + \rho_b)^2}\frac{P_b \bar{x}_{ab}^{\alpha}.\nabla_a W_{ab}}{|r_{ab}|^2 + \eta^2}\right) / \lambda\left(\sum_b \frac{8m_b}{(\bar{\rho}_a + \rho_b)^2}\frac{\bar{x}_{ab}^{\alpha}.\nabla_a W_{ab}}{|r_{ab}|^2 + \eta^2}\right) \tag{32}$$

where λ=1.1, is a relaxation factor can led to suitable results for simulation of a slender elastic structure. The amount of this factor for the fluid particles is one. These pressures are used to calculate the velocity field which is needed to restore the density of particles to their original value and finally the velocity of each particle at the end of time-step will be obtained.

$$\bar{u}_a^{\alpha} = -\Delta t \sum_b m_b \left(\frac{P_a}{\bar{\rho}_a^2} + \frac{P_b}{\rho_b^2}\right)\nabla_a W_{ab} \tag{33}$$

$$u^{\alpha}_{t+\Delta t} = \bar{\bar{u}}^{\alpha} + \bar{u}^{\alpha} \tag{34}$$

This velocity is smoothed according to the XSPH averaging of J.J. Manoghan [18] where $0 \le \xi \le 1$ is XSPH coefficient.

$$\breve{u}_a^{\alpha} = u_a^{\alpha} + \xi \sum_b \frac{2m_b}{\rho_a + \rho_b}\left(u_b^{\alpha} - u^{\alpha}_{t+\Delta t,a}\right)W_{ab} \tag{35}$$

Final positions of the particles are calculated using a central difference scheme in time:

$$x_t^{\alpha} = x^{\alpha}_{t-\Delta t} + \frac{\Delta t}{2}\left(\breve{u}_a^{\alpha} + u^{\alpha}_{t-\Delta t}\right) \tag{36}$$

V. TEST CASES

A. Collapse of water column with a rigid obstacle

Before starting with challenging elastic problems, a well known example of FSI benchmark problem is discussed to show the ability of the aforementioned algorithm. The initial geometry is illustrated in Fig. 1.

Gravitational force acts downwards with g=9.81 m/s^2 and air is neglected in simulations. Density and viscosity are respectively equal to 1000 kg/m^3 and 0.001 kg/ms.

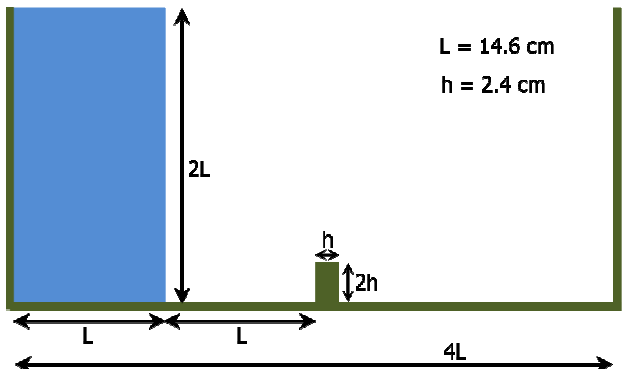

Fig. 1 Initial geometry of the water column and rigid wall

ISBN: 978-988-19251-5-2
ISSN: 2078-0958 (Print); ISSN: 2078-0966 (Online)

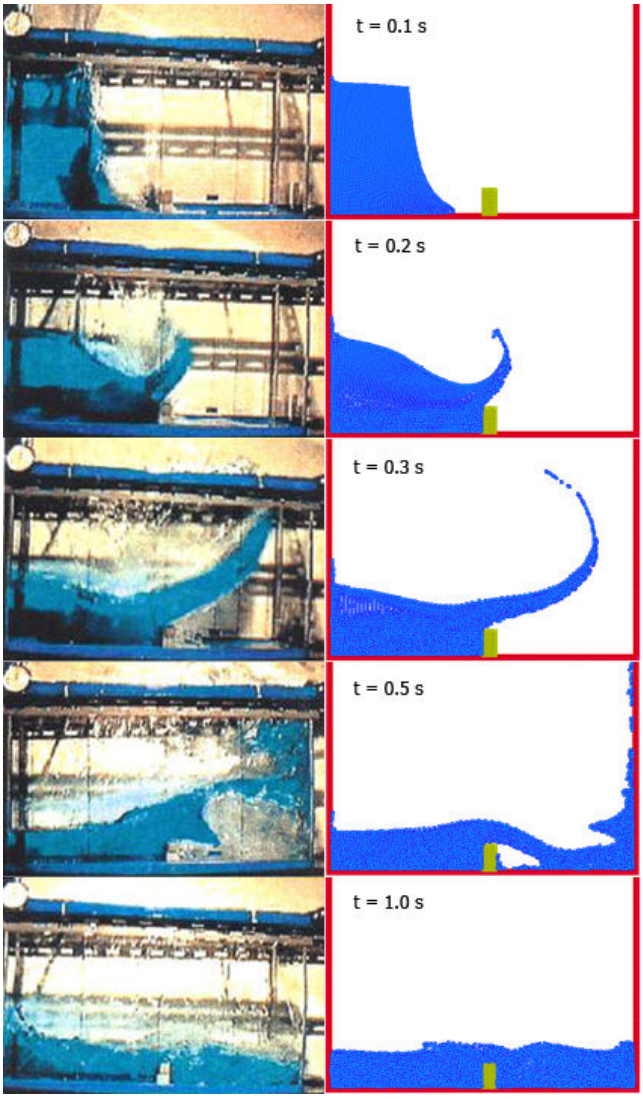

Fig. 2 Comparison of water profile of experimental results with SPH simulations for collapsing water column with obstacle

SPH results are compared with experimental results at different time steps (Fig. 2) obtained by S. Koshizuka in reference [19].

B. Breaking dam on a hypoelastic baffle

Fig. 1 represents the same problem but with a hypoelastic baffle with density 2500 kg/m^3, Young modulus 10^6 N/m^2 and the Poisson ratio of 0.0. The geometry of the more slender obstacle is of width b=1.2 cm and height (20/3)b. The time history of the displacement of the upper left corner of the baffle is compared with other available numerical results [9,20,21] and is illustrated in Fig. 3. No experimental results were found for this problem.

C. Bar under a lateral wave

In this example a bar is located in the middle of a tank. The obstacle has density 7800 kg/m^3, Young modulus $2.1*10^6$ and Poisson ratio 0.3.

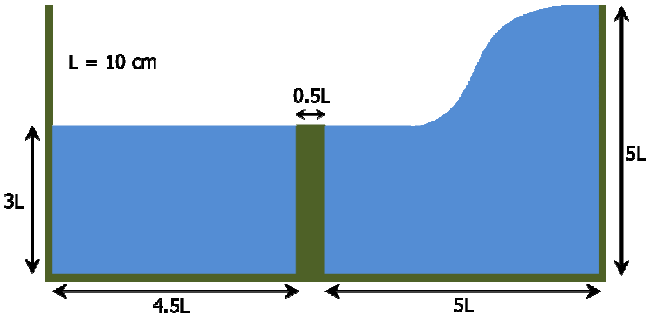

Fig. 4 Initial geometry of the bar under a lateral wave

The hypoelastic solid is deflected by the impulse of the fluid wave (Fig. 5). The solid first moves to the left while the water rises and to the right when the wave goes back.

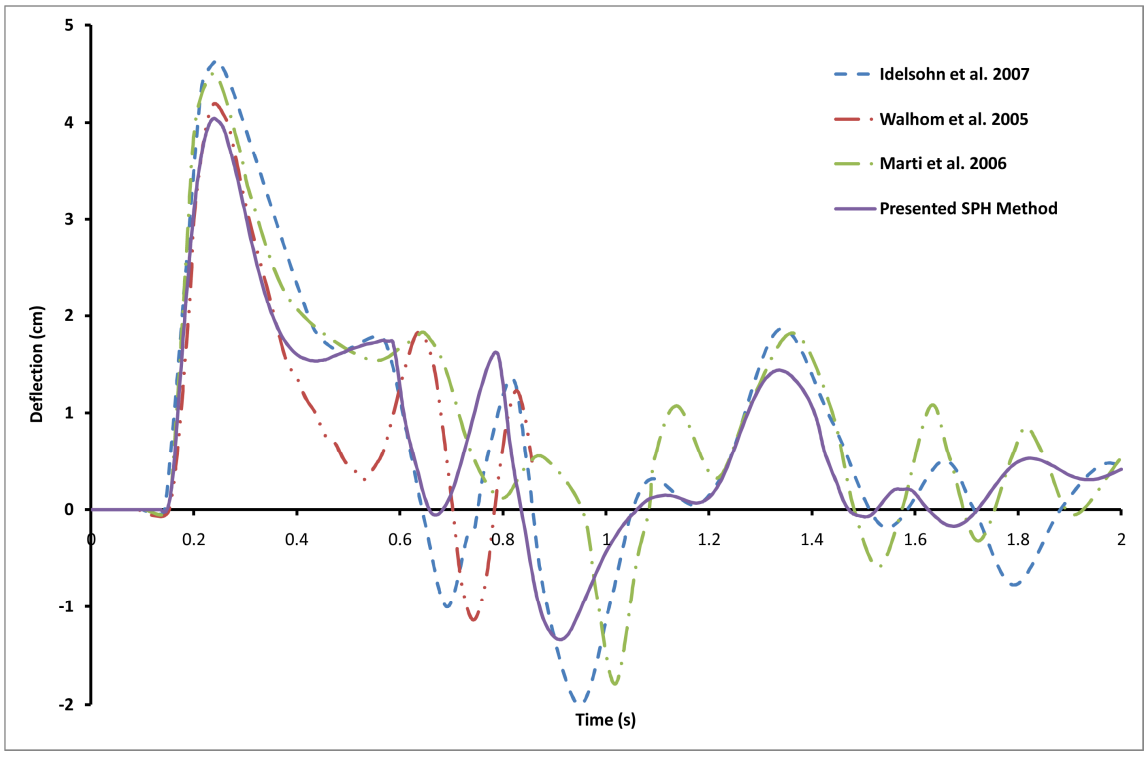

Fig. 3 Comparison between numerical results for time history of the displacement of the upper left corner of the baffle

ISBN: 978-988-19251-5-2
ISSN: 2078-0958 (Print); ISSN: 2078-0966 (Online)

SPH results at different time steps are compared with PFEM results reported by Marti *et al.* [20] in Fig.5. No experimental results were found for this problem.

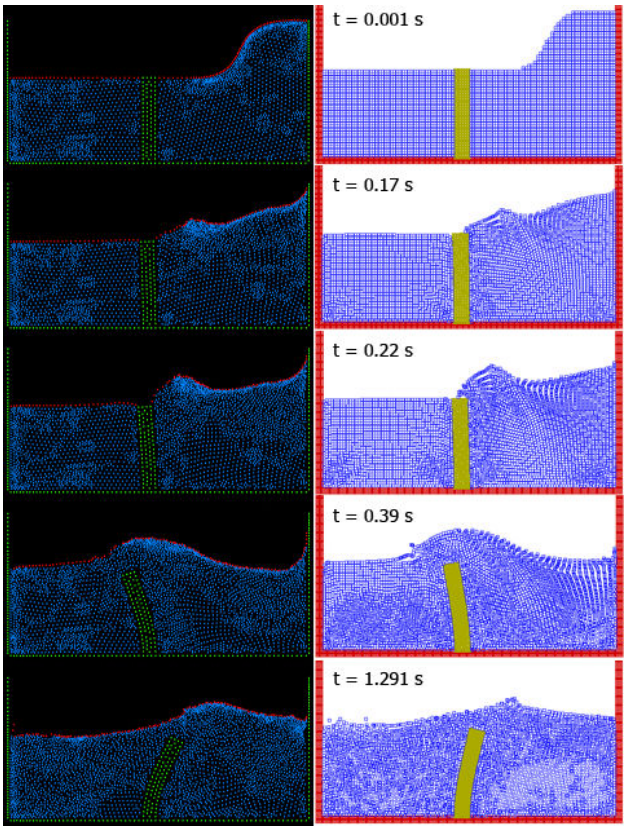

Fig. 5 Comparison of water profile of SPH results with PFEM simulations for bar under a lateral wave

REFERENCES

[1] T. Belytschko, W. K. Liu, B. Moran, "Finite elements for continua and structures," *John Wiley and Sons, New York.*

[2] U. M. Hans, "Review: hydrocodes for structure response to underwater explosions," *Shock and Vibration.* vol. 6(2), pp. 81–96, 1999.

[3] D. J. Benson, "Computational methods in Lagrangian and Eulerian hydrocodes," *Computer Methods in Applied Mechanics and Engineering.* vol. 99, pp. 235–394, 1992.

[4] L.B. Lucy, "A numerical approach to the testing of the fission hypothesis," *J. Astron.,* vol. 82, pp. 1013–1024, 1977.

[5] R.A Gingold, J.J. Monaghan, "Smoothed particle hydrodynamics: theory and application to non-spherical stars," *Mon. Not. R. Astron. Soc.,* vol. 181, pp. 375–389, 1977.

[6] J. J. Monaghan, "Smoothed particle hydrodynamics," *Ann. Rev. Astron. Astrophys.* vol. 30, pp. 543–574, 1992.

[7] J. J. Monaghan, "Smoothed particle hydrodynamics," *Rep. Prog. Phys.*, vol. 68, pp. 1703–1759, 2005.

[8] C. Antoci, M. Gallati, S. Sibilla, "Numerical simulation of fluid–structure interaction by SPH," *Computers and Structures*, vol. 85, pp. 879–890, 2007.

[9] S.R. Idelsohn, J. Marti, A. Limache, E. Onate, "Unified Lagrangian formulation for elastic solids and incompressible fluids: Application to fluid-structure interaction problems via the PFEM," Computer methods in applied mechanics and enginerring, vol. 197, pp. 1762-1776, 2008.

[10] J. P. Morris, P. J. Fox, Y. Zhu, "Modeling low Reynolds number incompressible flows using SPH," *J. Comp. Phys.* Vol. 136, pp. 214–226, 1997.

[11] J. J. Monaghan, J. C. Lattanzio, "A refined particle method for astrophysical problems," *Astronomy and Astrophysics,* vol 149, pp. 135-143, 1985.

[12] J. Gray, J. J. Monaghan, R. P. Swift, "SPH elastic dynamics," *Comput. Methods Appl. Mech. Eng.* vol. 190, pp. 6641–6662, 2001.

[13] S. J. Cummins, M. Rudman, "An SPH projection method," *J. Comput. Phys.,* vol 152 (2), pp. 584–607, 1999.

[14] E. Y. M. Lo, S. Shao, "Simulation of near-shore solitary wave mechanics by an incompressible SPH method," *Applied Ocean Research*, vol. 24, pp. 275–286, 2002.

[15] M.H. Farahani, N. Amanifard, G. Pouryoussefi, "Numerical simulation of a pulsatory flow moving through flexible walls using smoothed particle hydrodynamics," WCE London UK, vol II, 2008.

[16] S. M. Hosseini, N. Amanifard, "Presenting a modified SPH algorithm for numerical studies of fluid-structure interaction problems," *IJE Trans B: Applications*, vol. 20, pp. 167-178, 2007.

[17] S. M. Hosseini, M. T. Manzari, S. K. Hannani, "A fully explicit three step SPH algorithm for simulation of non-Newtonian fluid flow, " *Int. J. of Numerical Methods for Heat and Fluid Flow*, vol. 17, pp. 715–735, 2007.

[18] J.J. Monaghan, "On the problem of penetration in particle methods," *J. Comput. Phys.*, vol. 82, pp. 1–15, 1989.

[19] S. Koshizuka, H. Tamko, Y. Oka, "A particle method for incompressible viscous flow with fluid fragmentation," *Comp. Fluid Dyn. J.,* vol 4 (1), pp. 29–46, 1995.

[20] J. Marti, S.R. Idelsohn, A. Limache, N. Calvo, J. D'Ella, "A fully coupled particle method for quasi-incompressible fluid-hypoelastic structure interactions," *de Mecanica Computational*, vol xxv, pp. 809-827, 2006.

[21] E. Walhorn, A. Kolke, B. Hubner, D. Dinkler, "Fluid–structure coupling with monolithic model involving free surface flows," *Comp. Struct.* vol 83, pp. 2100–2111, 2005.

ISBN: 978-988-19251-5-2
ISSN: 2078-0958 (Print); ISSN: 2078-0966 (Online)